Materials Research. 2025; 28(suppl. 1):e20250180
DOI: https://doi.org/10.1590/1980-5373-MR-2025-0180

Multilayer Strategies Incorporating Natural Bactericide for Titanium Surface Functionalization

***Carolina Cruz Ferreira*[a,b*], *Ingrid Zavarize Evangelista Vieira*[b], *Carla Sérgio Barboza*[b],**

***Andrés Vercik*[c], *Luci Cristina de Oliveira Vercik*[c], *Daniela Sachs*[d], *Neide Aparecida Mariano*[b]**

[a]*Universidade Estadual de Campinas (UNICAMP), Faculdade de Engenharia Química, Campinas, SP, Brasil.*
[b]*Universidade Federal de Alfenas (UNIFAL), Instituto de Ciência e Tecnologia, Poços de Caldas, MG, Brasil.*
[c]*Universidade de São Paulo (USP), Faculdade de Zootecnia e Engenharia de Alimentos, Pirassununga, SP, Brasil.*
[d]*Universidade Federal de Itajubá (UNIFEI), Instituto de Física e Química, Itajubá, MG, Brasil.*

Received: January 24, 2025; Revised: April 12, 2025; Accepted: April 21, 2025

Current development of hybrid and bioactive materials based on consolidated metallic substrates, such as titanium and its alloys, combined with polymeric and ceramic additives has been promoted. These materials, with an emphasis on hydroxyapatite and polycaprolactone, have a high applicability in tissue replacement and regeneration. Since bacterial contamination and biofilm formation are the main causes of post-surgical complications involving implants, the present work proposes a hybrid coating to address these issues. It incorporates *Melaleuca alternifolia* essential oil as a natural bactericide, into a polymeric PCL layer. This layer was applied over a bioceramic coating on a commercially pure titanium substrate. The surface evolution of the apatite layer was verified through bioactivity tests in simulated body fluid, verifying a homogeneous layer with appreciable globular morphology. In the microbiological assays by disk-diffusion against *Staphylococcus aureus* and *Escherichia coli*, the formation of small halos was observed for both cultures. As a result, it is suggested that the proposed hybrid coating may improve the osseointegration process and biocompatibility, indicating the potentiality of prosthetic application in orthopedic medical devices.

Keywords: *Titanium, Polycaprolactone, Hydroxyapatite, Melaleuca alternifolia.*

1. Introduction

Several forms of natural or synthetic biomaterials have been noted as potentially relevant for boosting the tissue regeneration effectiveness of traditional metallic substrates, such as titanium and its alloys, applied in the manufacture of medical devices. Among them, the bioceramic material hydroxyapatite (HA) is remarkable because it is highly accepted by biological systems and effective in repairing bone defects, the polycaprolactone (PCL), a biodegradable synthetic polymeric material recognized for versatility and the formation of biocompatible coatings[1-9].

One of the major challenges of any medical procedure is the prevention and control of infection, especially for replacement surgeries, which are considered the most invasive and vulnerable to contamination. So the main causes of post-operative problems in implant operations are bacterial adherence to implants and biofilm formation[10-17].

Up to 80% of human bacterial infections, according to the National Institutes of Health (NIH), are driven on by bacterial biofilms. Treatment can be difficult if implants are involved because of the hard diagnosis. The most common protocol treatment in these situations involves giving high doses of antibiotics or implanting another device, both of which are ineffectual and have a strong probability of reinfecting the new implant[10-12,18].

Bacterial biofilms are notoriously difficult to treat because they are highly resistant to both antibiotics and the human immune system. Despite this, synthetic antibiotics, which can have serious negative side effects, are still used in conventional processes of infection prevention and treatment. Thus, treatments based on non-conventional antibiotics are attractive due to their multiple actions against microorganisms and less adverse effects than synthetic medicines, reducing the development of drug-resistant bacteria[10,12,18-22].

A promising strategy that can prevent the first adhesion of pathogens to the implant surface is the incorporation of bactericidal and antibiofilm agents in the coatings of the materials to be implanted. Beyond the consolidated metallic nanoparticles, the use of essential oil-based antimicrobial coatings is a desirable method for greatly improving their biocompatibility and preventing microbiological growth on

*e-mail: carolcruzf@gmail.com

implant surfaces, once the biocidal activity of such coatings seems to be restricted to bacteria, allowing mammalian cells to attach and proliferate well[12-17,21].

Compared to synthetic medications, essential oils can work at the same time on several target molecules, in addition to being natural and biodegradable. *Melaleuca alternifolia* essential oil, generally known as tea tree essential oil (TTO) has been explored as a potential antibacterial and antifungal additive to be included in polymeric coatings. Terpinen-4-ol and 1,8-cineol, which make up the majority of its complex mixture of terpene hydrocarbons and tertiary alcohols, are the compounds responsible for its documented analgesic and anti-inflammatory effects, as well as the exceptional antimicrobial activity of TTO across a wide spectrum, both *in vitro* and *in vivo*[23-29].

In this regard, the current work proposes a surface-modifying of commercially pure titanium (Ti c.p. grade 4) by the incorporation of TTO as a bactericidal agent into a PCL-based dip coating applied to the metallic substrate, as well as the effect of prior HA coating on the titanium surface. With the selected compounds, aim to develop a hybrid functional material with higher bioactivity while simultaneously lowering the risk of post-surgical contamination, making them promising coatings components and potential for use in prosthetics manufacture.

Despite preliminary work[21], the hybrid coating was structurally characterized previously, demonstrating that them improve implant surface protection against bodily fluid attack. In order to verify the effects of proposed coatings on bioactivity, the apatite-forming capacity was examined by immersing the samples in simulated body fluid (SBF) for up to 4 weeks and following up with inspection by employing a Scanning Electron Microscope (SEM), Energy Dispersive Spectroscopy (EDS), and Fourier Transform Infrared Spectroscopy (FTIR). Antimicrobial activity of the proposed system has been tested using the disk-diffusion method against gram-positive *Staphylococcus aureus* (*S. aureus*) and gram-negative *Escherichia coli (E. coli*). The resulting hybrid coatings created on Ti c.p. surfaces displayed good bioactive capabilities and antimicrobial activity, suggesting that they are a viable strategy for enhancing titanium-substrate implant properties and, simultaneously, minimizing implant-associated infections and promoting osteointegration of orthopedic devices.

2. Materials and Methods

Titanium alloy samples previously coated with HA by the biomimetic method were used, followed by PCL coating containing incorporated TTO, according to the steps described below.

2.1. Materials

Samples of Ti c.p. disks grade 4 (3 mm in diameter and 5 mm in thickness) were used as metallic substrate. Table 1 presents the chemical composition of the samples, determined by inductively coupled plasma optical emission spectrometry (ICP-OES), together with the values stipulated by ASTM F67-0630[30].

For the polymeric coating, PCL (Sigma Aldrich; Mn 70000–90000, density 1.145 g/mL at 25ºC) was employed, together with TTO (Phytoterápica; Lote POM17.05). The acellular solution of simulated body fluid (SBF) applied in the steps of biomimetic coating and in the bioactivity assay was prepared as stated in the standard ISO 23317:2014[31], according to the concentrations shown in Table 2.

2.2. Sample preparations

The surface of the Ti c.p. substrate was prepared passing through a 180 mesh sandpaper. Then, the samples were placed in an ultrasonic bath with detergent, distilled water and isopropyl alcohol, for 15 minutes in each solution, for the removal of impurities. Previous works has shown that such sample preparation conditions favor the creation of surface defects, enabling the adhesion of coatings[20-22,32,33].

Subsequently, it was immersed in a 5M NaOH solution (alkaline treatment) and placed in an oven at 60ºC for 24 h. After the alkaline treatment, the disks were washed with distilled water, dried and subjected to thermal treatment in an oven at 600ºC for 1 hour and cooled at room temperature in a desiccator. These pretreatments help to increase the substrate's surface's bioactivity by modifying its roughness, creating nucleation sites, and depositing a thin coating of Na_2O-TiO_2, which stimulates the formation of a denser apatite[34].

2.3. Biomimetic coating

By using the two-stage (nucleation and growth) biomimetic technique, some samples were coated with HA. The samples were immersed in a solution of $2x10^{-3}$ mol/L of sodium silicate during the nucleation stage at 36.5 °C for seven days before being dried in a desiccator at ambient temperature. During the growth phase, the samples were submerged in SBF solution (previously prepared) for seven days at 36.5 °C, replacing it with a fresh solution every 48 h to ensure medium supersaturation and promote the creation of the HA layer.

Table 1. Chemical composition of Ti c.p. (in % wt).

Chemical Element	ASTM F67-06[30]	Ti c.p.
N	0.030 (max)	0.006
C	0.100 (max)	0.090
H	0.015 (max)	0.013
Fe	0.200 (max)	0.110
O	0.180 (max)	0.140
Ti	balance	balance

Table 2. Ionic concentrations of SBF solution ($mmol.dm^{-3}$).

Ion	Concentration
Na^+	213.00
K^+	7.50
Ca^{2+}	3.75
Mg^{2+}	2.25
HCO_3^-	6.30
HCl^-	221.70
HPO_4^{2-}	1.50
SO_4^{2-}	0.75

Following this time, the Ti disks were cleaned with distilled water and dried in a desiccator at 25ºC .

2.4. PCL coating containing TTO

Afterward, the coating with PCL containing the essential oil was performed by the dip coating method. A polymeric solution at the concentration of 5% (m/v) was prepared dissolving the polymer in chloroform under magnetic agitation. Then, the TTO was incorporated in a concentration of 2% in relation to the polymer mass, dripping it in the solution still under magnetic agitation, at 800 rpm in a magnetic stirrer . The samples were coated with PCL containing TTO, by the immersion in the polymeric solution for 3 seconds, repeating the process 3 times, and then they were dried at 25ºC in the desiccator for 24 h. So, the uncoated condition was named Ti c.p., the samples containing previously HA coating were named Ti+HA+PCL+TTO, while the others without HA coating were named Ti+PCL+TTO.

2.5. Bioactivity assays

The apatite-forming ability of the implant material was evaluated using the bioactivity test, following the ISO 23317:2014[31] standard. This test measures the formation of apatite over four weeks and serves as a preliminary method to predict the material's in vivo bone-bonding potential. Ti c.p. coated samples were immersed in SBF solution for four weeks at 36.5 °C, with weekly evaluations conducted throughout the test. After this time, the samples were cleaned with distilled water and dried in a desiccator.

In order to determine the growth of apatites, the surface of the samples was evaluated by scanning electron microscopy (SEM) and energy dispersive spectrometry (EDS), performed in the microscope (FEI, model Inspect S50) coupled to an EDA detector (EDAX, model Apollo X), with the samples fixed with carbon tape. The functional groups present in the samples were analyzed by Fourier transform infrared spectroscopy (FTIR), using a spectrometer (Perkin Elmer, model Spectrum 100 FTIR Spectrometer) with attenuated total reflectance accessory (ATR), employing a zinc selenide (ZnSe) crystal. The spectra were performed in the range from 450 to 4000 cm^{-1}, with 32 scans and "background" of the measures employing the crystal without the sample.

2.6. Bacterial assays

To evaluate the antimicrobial potential of the samples, the disk diffusion method was used, testing the proposed conditions for the bacterial strains *Staphylococcus aureus* (ATCC 6538) and *Escherichia coli* (ATCC 8739). Bacteria were suspended in a 0.9% NaCl solution up to scale 0.5 of McFarland (108 cells mL^{-1}) and seeded on the surface of Muller-Hinton agar plates with the aid of sterile swabs. Samples were placed under bacterial culture and incubated for 24 h at 37º C. Each Petri dish received a filter paper disk containing chlorhexidine as the positive control, filter paper disk as the negative control, Ti c.p. uncoated (without any coating, only pre-treated) and Ti c.p coated disks. The diameter of the halo formed around the disks was measured according to the Clinical and Laboratory Standards Institute (CLSI)[35] guidelines for disk-diffusion sensitivity tests. Statistical analyses were performed using analysis of variance (ANOVA) and Tukey post hoc test to. Values were expressed as the mean±standard error with n=3 and $P<0.05$ as significant level.

3. Results and Discussion

3.1. Bioactivity assays

The micrographs obtained by SEM for the coated samples before the bioactivity test are shown in Figure 1. It is possible to observe that the coating was carried out homogeneously over the entire surface of the metallic substrate, as reported in previous works[21]. For the Ti+PCL+TTO sample (Figure 1a), the presence of bubbles resulting from

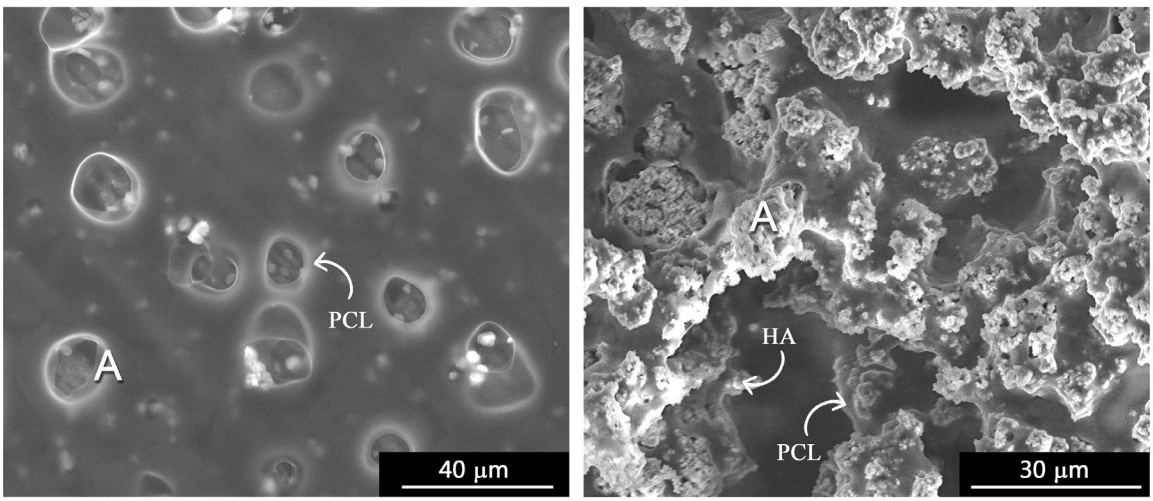

Figure 1. Micrographs obtained by SEM of the samples: (a) Ti+PCL+TTO e (b) Ti+HA+PCL+TTO.

the evaporation process of the solvent used in the polymeric solution is noted as observed by Ferreira et al.[21], while for the Ti+HA+PCL+TTO condition (Figure 1b) it is possible to visualize a porous granular region and homogeneous layers with small globules characteristic of the presence of HA. As previously observed by Ferreira et al.[21], there was no influence on the performance of the samples in corrosion tests using SBF, despite the bubbles present in the coating.

The semiquantitative microanalysis by EDS carried out in region A identified the atomic percentage of the chemical elements for each condition. The composition (in at%) of the samples is shown in Table 3. The presence of C and O refers to the existence of PCL and TTO coating, Ca and P components indicate the HA layer, while Na and Cl derives from the reagents (NaOH, NaCl, KCl, $MgCl_2.6H_2O$, $CaCl_2.Na_2SO_4$, $NaHCO_3$ and HCl) used in the preparation of the biomimetic coating, according to Table 2.

The essential condition for implants to bond to bone under *in vivo* conditions is the formation of a surface layer of biologically active apatite like the bone component. When the bioactive material is implanted, a series of biochemical and biophysical reactions are triggered between the implant and the contact tissue, resulting from a strong interfacial interaction associated with the superficial formation of a thin layer with a high concentration of Ca and P[36,37]. In addition, surface porosity is also a desired property for bone tissue substitute devices, as it favors the transfer of nutrients, endogenous cell migration and, consequently, promotes bone growth[38,39].

The characteristics of the bioactivity of the Ti+PCL+TTO samples are shown in micrographs obtained by SEM (Figure 2) during the four weeks of the assay. Through them, it is possible to observe the metallic substrate matrix (darker region), together with the formation of porous mineralization nodules (lighter region). It is possible to visualize that the apatite grows from the first week, presenting a rounded globular structure favorable to the osseointegrative process.

At the end of the 4 weeks of testing, it is possible to verify the presence of overlapping layers of apatite, filling a large portion of the metallic substrate and forming larger clusters than those observed in the first week. Furthermore, it is observed that the bubbles resulting from the drying of the polymeric coating as well as the metallic substrate are more evident in the first week micrograph (Figure 2a), suggesting the possible degradation of the PCL+TTO coating simultaneously with the growth of the apatite layers.

Table 3. Chemical composition (%at) obtained by EDS microanalysis in the A region.

Chemical Element	Ti+PCL+TTO	Ti+HA+PCL+TTO
Ti	1.01	0.12
C	86.92	35.88
O	12.07	19.96
Ca	N/A	21.87
P	N/A	13.02
Na	N/A	1.23
Cl	N/A	7.92
Ca/P ratio	**N/A**	**1.68**

The surface evolution of the Ti+HA+PCL+TTO samples over the four weeks of bioactivity is depicted in Figure 3 through the micrographs obtained by SEM. For this condition, it was possible to observe that the apatitic growth occurs faster than in the Ti+PCL+TTO system. After immersion in SBF solution for a week, it is already possible to verify the formation of larger compact clusters than observed for the previous system, favored by the previous presence of HA coating.

There is also an overlapping of layers over the weeks, so that the inner layers have globules with a smaller diameter than those present in the outer layers, since their growth will be constrained by the subsequent layers. In addition to the evident stacking, it was possible to observe the globular morphology of the apatite coating, which is a notable aspect of the osseointegrative process.

The structure of the systems coated after immersion in SBF can be seen in greater detail in Figures 4 and 5. To confirm the chemical composition, microanalysis by EDS was carried out in regions B. For the Ti+PCL+TTO sample, the composition (in %at) after the first week and the fourth week of testing is shown in Table 4. The presence of Ca, and P components denote the apatite layer, while Mg, Na, K and Cl descends from the reagents used in the preparation of the SBF (NaOH, NaCl, KCl, $MgCl_2.6H_2O$, $CaCl_2.Na_2SO_4$, $NaHCO_3$ and HCl), according to Table 2.

After four weeks of testing, there is a reduction in the percentage of Ti, corroborating what was observed by the micrographs since the layers of apatite formed overlap, extending throughout the metallic substrate. The reduction in the amounts of Ca and P can be explained by the presence of additional elements deposited on the surface, which may be in higher concentration at the point where the analysis was performed. The evaluation of the Ca/P ratio of the Ti+PCL+TTO samples after the bioactivity test will be further discussed in a later section, after the presentation of the SEM micrographs and EDS microanalysis, in order to facilitate the comparative analysis with the other conditions studied.

For the system containing HA (Ti+HA+PCL+TTO), through EDS microanalysis in the C region, the composition (in %at) after the first week and the fourth week of testing is shown in Table 4. Larger globules are seen in this condition during the first week (Figure 5a). Despite the slight variation between the amount of Ti detected after the first and fourth weeks, there is a decrease of approximately 50% compared to the composition before the bioactivity assay (Ti = 0.12%at), justified by the density of the apatite layer formed.

The bioactivity of uncoated Ti c.p was analyzed by por Coelho et al.[33], in which the authors reported that the formation of HA did not occur in the first week, with the development of apatite globules occurring only in subsequent weeks, in contrast to what was obtained for the coated materials proposed in the present work.

To compare the effect of TTO, a bioactivity assay was performed on the Ti c.p. covered only with PCL, and the micrographs obtained by SEM and the spectra by microanalysis by EDS are shown in Figure 6. The composition (in %at) obtained by means of the microanalysis by EDS performed in region D was C (9.52), O (56.54), Na (4.81), Mg (1.08), P (2.17), Ca (10.01), and Ti (15.87) for the first week, and C

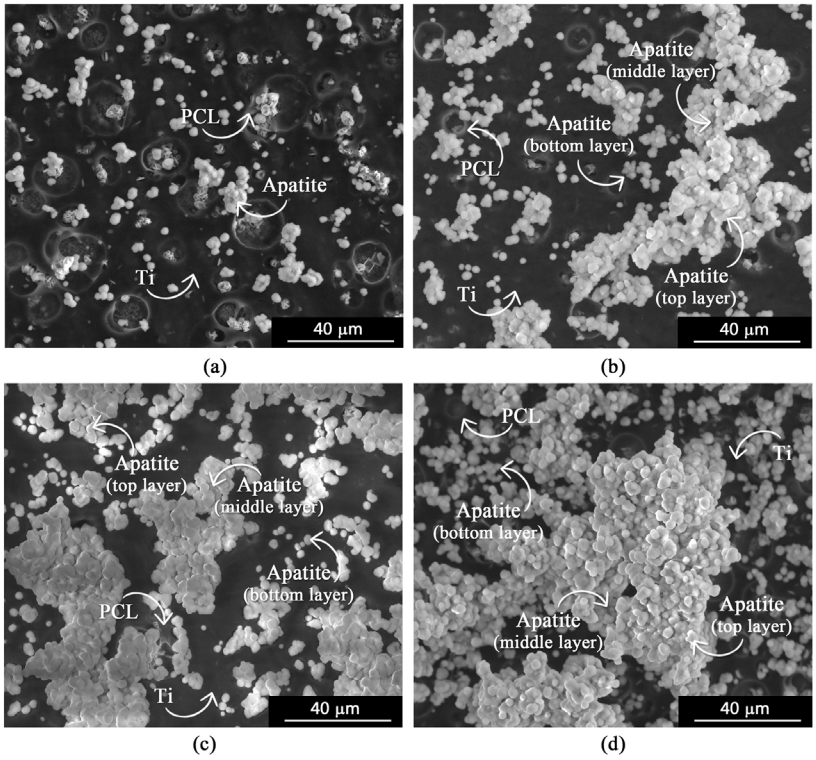

Figure 2. Micrographs obtained by SEM for the Ti+PCL+TTO sample, after bioactivity assay. (a) first week, (b) second week, (c) third week, and (4) fourth week.

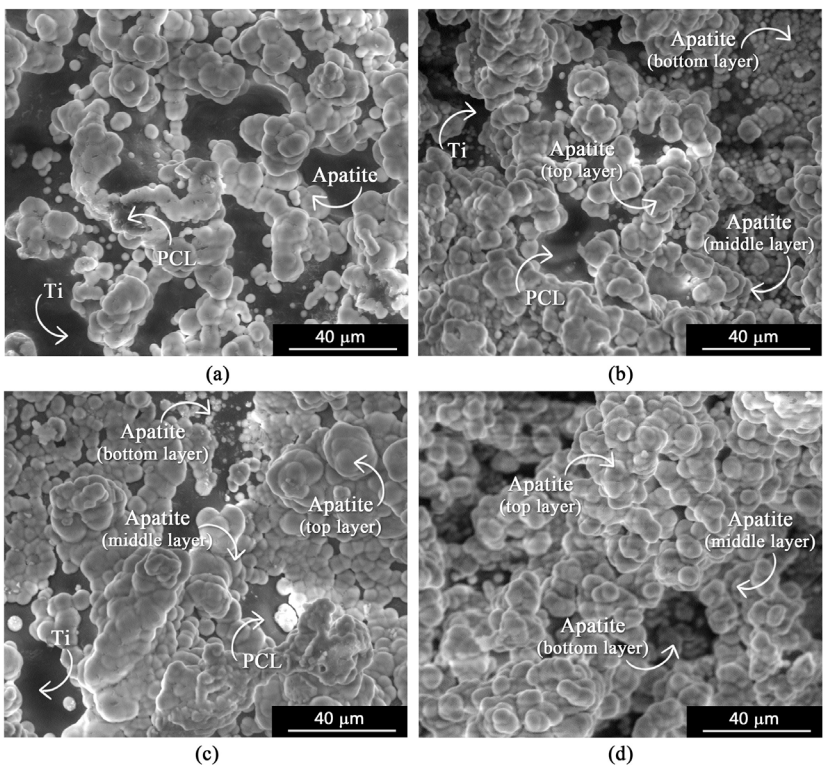

Figure 3. Micrographs obtained by SEM for the Ti+HA+PCL+TTO sample, after bioactivity assay. (a) first week, (b) second week, (c) third week, and (4) fourth week.

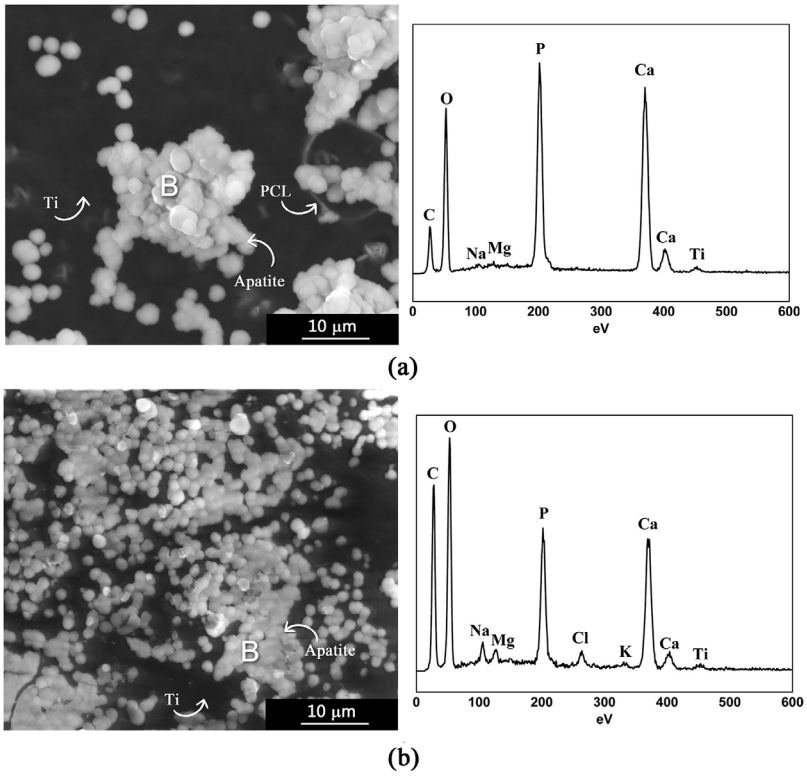

Figure 4. Micrographs obtained by SEM and EDS microanalysis spectra in the B region, for bioactivity assay of the Ti+PCL+TTO sample after (a) first week; (b) fourth week.

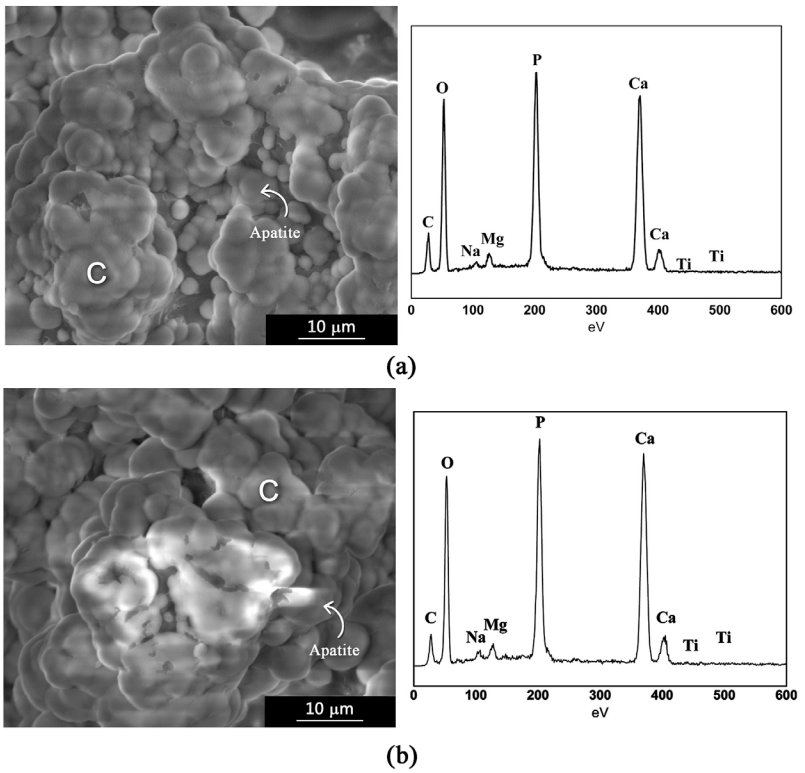

Figure 5. Micrographs obtained by SEM and EDS microanalysis spectra in the C region, for bioactivity assay of the Ti+HA+PCL+TTO sample after (a) first week; (b) fourth week.

Table 4. Chemical composition (%at) obtained by EDS microanalysis for bioactivity assay of the samples after first and fourth week.

Chemical Element	Ti+PCL+TTO		Ti+HA+PCL+TTO	
	1st week	4th week	1st week	4th week
Ti	1.35	0.46	0.06	0.05
C	20.16	42.33	17.17	12.31
O	46.56	39.83	49.61	54.06
Ca	18.68	8.99	18.68	20.75
P	13.35	5.70	13.20	14.01
Na	0.37	1.02	0.42	0.86
Mg	0.27	0.57	0.86	0.97
K	N/A	0.33	N/A	N/A
Cl	N/A	0.78	N/A	N/A
Ca/P ratio	**1.40**	**1.58**	**1.41**	**1.48**

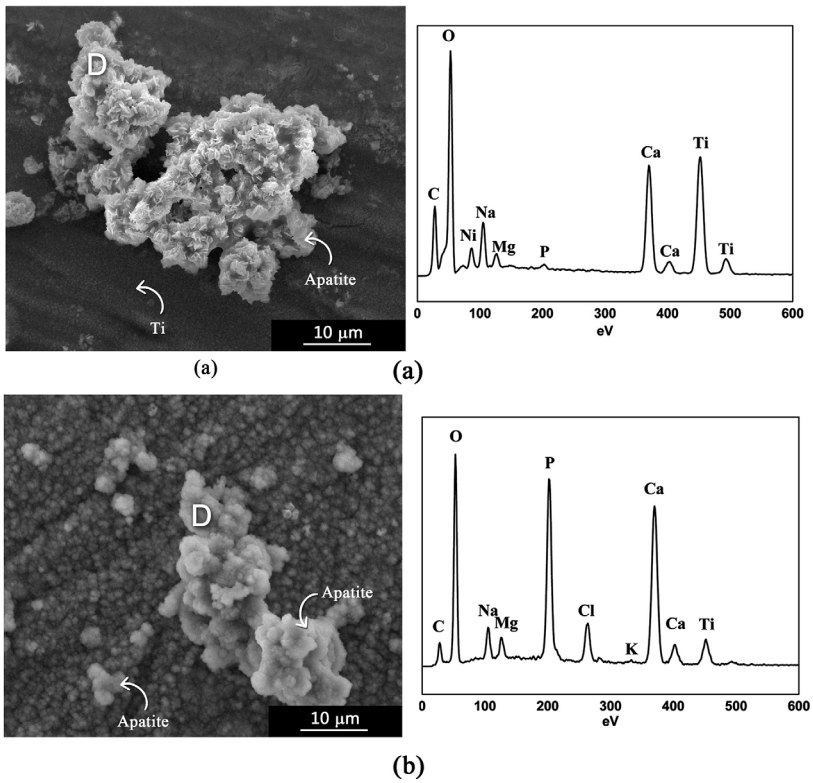

Figure 6. Micrographs obtained by SEM and EDS microanalysis spectra in the D region, for bioactivity assay of the Ti+PCL sample after (a) first week; (b) fourth week.

(5.72), O (52.18), Na (3.02), Cl (3.31), Mg (1.55), P (12.88), Ca (17.76), and Ti (3.57) after the fourth week of testing.

Without TTO, apatite growth is detected to occur in the first week, but with needle-like structures, as observed by Coelho et al.[33] that are unfavorable to subsequent bone-implant integration. After the fourth week of testing, the presence of a primary apatite layer at the bottom is noted, superimposed by thicker layers. However, the globules in the upper layers changed in morphology, with loss of pore limitations and contour definition, as observed by Costa et al.[40] in sheep tibia samples implanted to repair a proximal bone defect.

A similar apatite structure was observed by Ferreira et al.[20] for the coating containing PCL+$AgNO_3$. It is therefore suggested that TTO also acts on the growth of apatites, favoring their morphology for the osteointegrative process. Studies conducted by Alves et al.[41] confirmed the cell viability of scaffolds containing TTO for osteoblast-like MG-63 cells. This effect is possibly due to the presence of components such as 1,8-cineol, α-pineno, α-terpineol e γ-terpineno, also found in essential oils used in studies conducted by Sabbieti et al.[42] and Elbahnasawy et al.[43], which had positive effects on Ca absorption and osteoblast proliferation.

The association of PCL with calcium phosphates (CaP) to create a hybrid material is one of the approaches applied to improve the bioactive properties of the polymeric matrix, since it was verified that the similarity with the mineral composition of the bone tissue and the osteoconductive properties of the CaP can promote cell attachment and proliferation *in vitro*, as observed by Gorodzha et al.[44].

From a commercial point of view, there are several CaPs applicable in bone replacement that have a Ca/P molar ratio between 0.5 and 2.0[45,46]. Like synthetic CaP, biogenic apatite from bone tissue also presents stoichiometric deviations in the Ca/P molar ratio, ranging from 1.33 to 1.77, as a result of possible ionic incorporation[45-47].

Evaluating the Ca/P ratio of Ti+PCL+TTO samples after the bioactivity assay (Table 4), there was an increase in this ratio from 1.4 to 1.58 from the first to the fourth week, resulting in an HA deficient in calcium (Ca/P between 1.5 and 1.67)[45,46].

According to previous studies[21], it is suggested that the development and growth of the apatite layer in the coated material is a dynamic process and that it occurs simultaneously with the degradation process of the polymeric coating. Once the PCL+TTO layer is solubilized, the metal substrate becomes more exposed to the SBF solution, triggering the formation of surface Ti–OH groups that stimulate apatite nucleation. Once the apatite nuclei are formed, growth occurs spontaneously, consuming positive calcium ions (Ca^{2+}) and negative phosphate ions (PO^{3-}) from the SBF fluid, which will spontaneously transform into hydroxyapatite[9,48]. It is then suggested that the Ca/P ratio of the Ti+PCL+TTO samples will increase over time, reaching the stoichiometric HA ratio of 1.67[45,46].

The Ca/P ratio (1.68), obtained prior to immersion of the samples Ti+HA+PCL+TTO in SBF medium for the bioactivity assay, confirms the presence of HA in the coating. Nevertheless, over the weeks of the bioactivity test (Table 4), this ratio changes, reducing to 1.41 after the first week, followed by an increase to 1.48 at the end of the fourth week. Such results suggest that the initial HA will undergo partial replacement of Ca in the apatite structure by Mg present in the SBF solution, as reported by Ferreira et al.[21], transforming into tricalcium phosphate (TCP), with a Ca/P molar ratio close to 1.5[45,46].

The β-phase of tricalcium phosphate (β-TCP) has been extensively investigated and used clinically due to its chemical composition similar to the apatite naturally present in bone tissue[47,49,50]. The combination of β-TCP with PCL has been considered a promising strategy for application in bone grafting because it is effective in bone regeneration in *in vivo* models, as reported by Lee et al.[51] for mandibular reconstruction in dogs and Chen et al.[49] for a rabbit bone defect model. Furthermore, as studies conducted by Helaehil et al.[52] demonstrated, the combination of β-TCP with PCL provides improved application to the PCL-HA association for long-term applications in relation to the bone regenerative process of critical size bone defects.

The evolution of HA presence can be verified through infrared analysis of absorption bands corresponding to the vibrations of phosphate, carbonate, and hydroxyl groups. Figure 7 compares the spectra obtained after the first and fourth weeks for the Ti+PCL+TTO (Figure 7a) and Ti+HA+PCL+TTO (Figure 7b) samples. The main peaks of interest were identified, to obtain a clearer visualization of the evolution of the bands over the bioactivity assay period.

Bands associated with OH^- group stretching were observed between 3670 and 3570 cm^{-1}, whereas bands associated with CO_3^{2-} group stretching were observed between 1514 cm^{-1} and 1412 cm^{-1}. Bands related to the phosphate group were identified at 1196 and 1022 cm^{-1} (stretching) and at 563 cm^{-1} (vibration). Comparing the intensity of the bands observed in the first and fourth weeks, a greater intensity is observed after the fourth weeks of testing, corroborating the HA growth observed by the micrographs for both proposed systems.

The characteristic bands of PCL and TTO were identified in the spectra, and also reported by Ferreira et al.[21,32]. The bands that correspond to the C=C bond in the aromatic ring (1670 cm^{-1}) and the elongation of the C-O bond (1160 cm^{-1}) are related to the presence of TTO in the coating. The bands

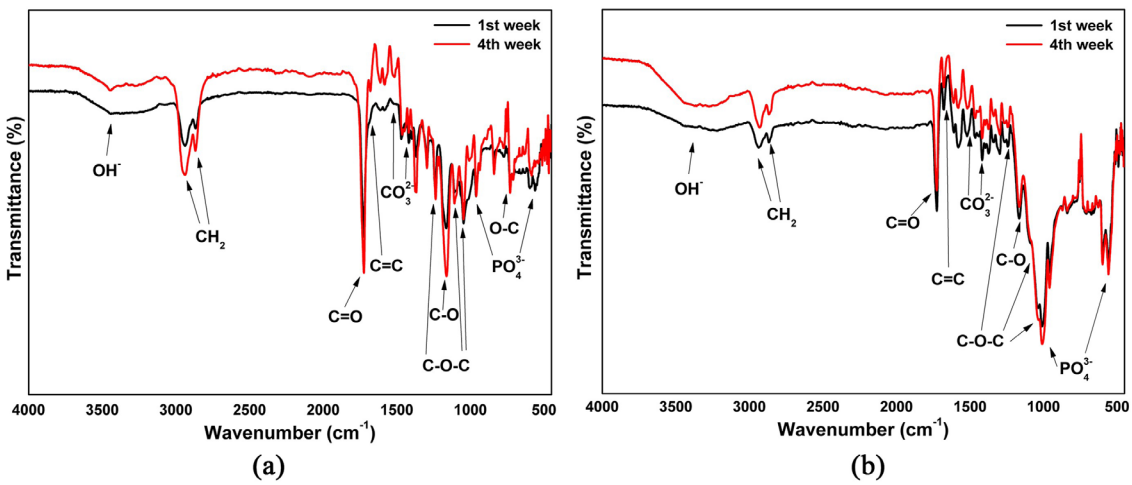

Figure 7. Infrared spectra obtained after the first and fourth weeks of bioactivity assay for the samples (a) Ti+PCL+TTO and (b) Ti+HA+PCL+TTO.

related to the asymmetric and symmetric elongation of the CH_2 bonds can be observed at 2900 cm^{-1}, while the elongation vibration of the carbonyl group (C=O) of the PCL ester function is observed at 1736 cm^{-1}. The wavelengths 1233, 1107, 1042, and 731 cm^{-1} are associated with the asymmetric vibrations of the C-O-C bonds, present in the amorphous phase of the polymer.

For both conditions, it is possible to observe that the bands associated with the existence of the PCL+TTO coating remained present after the four weeks of testing, suggesting that the coating was still adherent to the surface of the material.

Comparing the results obtained, it is noted that the samples previously coated with HA present faster growth during the bioactivity test, due to the presence of HA on the surface of the material. This was also observed by Valente et al.[53], who compared the efficacy of pure PCL and HA+PCL composites containing or not containing alendronate in the repair of bone defects in rabbit olecranon. Although all conditions studied showed biocompatibility and biodegradation capacity simultaneously with the formation of bone tissue, the response of composites containing bioceramic material (HA) was more evident.

3.2. Bacterial assays

The antibacterial activity of uncoated Ti c.p., Ti+PCL+TTO, and Ti+HA+PCL+TTO samples against *E. coli* and *S. aureus*, as examples of gram-negative and gram-positive bacteria, was investigated using the disk diffusion technique. The results obtained are displayed in Figure 8. Although it has drawbacks for the evaluation of liposoluble substances with a high degree of volatility, such as essential oils, the disk diffusion method can be used as a preliminary step for evaluating the antimicrobial activity of these substances[54].

According to the analysis of the curves, it is observed that the inhibition halos obtained for the Ti+HA+PCL+TTO condition in both evaluated bacteria are similar, with mean inhibition diameters of 6.67±0.058 mm (*S.aureus*) and 6.367±0.151 mm (*E.coli*). The Ti+PCL+TTO system expressed the highest inhibition halo against *S.aureus* strains (mean inhibition diameter of 7.70±0.142 mm), while the antibacterial activity against *E.coli* was slightly lower (mean inhibition diameter of 6.135±0.078 mm) than for the sample containing HA.

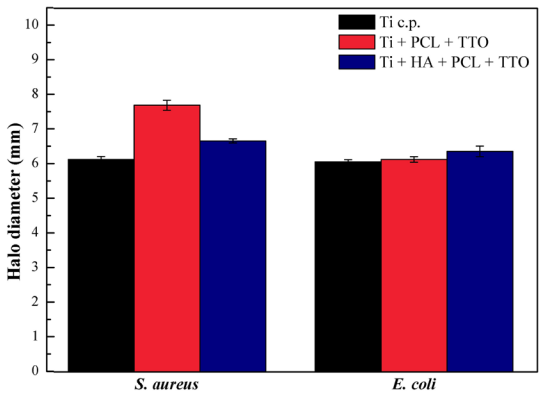

Figure 8. Mean of inhibition zone of samples against *E. coli* and *S. aureus* (disk-diffusion method).

The presence of halos in the uncoated condition (Ti c.p.) may occur due to the presence of surface TiO_2 naturally formed after alkaline and thermal treatments. For this condition, the mean diameter of the formed halos was 6.13±0.088 mm (*S.aureus*) and 6.067±0.058 mm (*E.coli*) were dimensionally similar to those obtained by Weng et al.[55] for TiO_2 samples.

TiO_2 is among the inorganic substances with recognized antimicrobial activity, originally due to its excellent photocatalytic activity. Its excellent antifungal and antibacterial properties against a wide range of gram-positive and gram-negative bacteria are reported by several authors[55-57] and are strategically applied in the coating of biomedical devices, in addition to being able to be satisfactorily associated with other polymers, such as PCL[9,48].

Mumu and Hossain[58] comparing the antimicrobial activity of various essential oils and found that TTO has a greater ability to prevent pathogens, inhibited 99.92% of pathogens after 6 h of incubation, while the other oils inhibited between 90.43 and 92.59%. Studies suggest that the mechanism of action of TTO results from an increase in the permeability of liposomal systems, causing lysis and loss of membrane integrity, denaturing the protein structure, and inducing the death of the bacteria[28,58,59].

Tests conducted by Singh et al.[59] demonstrated that TTO exhibits bacteriostatic behavior at low doses but develops bactericidal behavior at high concentrations. Differences in the susceptibilities of the tested organisms to TTO were also observed, and these are interpreted in terms of variations in the penetration rate of monoterpenes through the cell wall and cell membrane structures[28,59].

The addition of TTO offered inhibitory activity against both bacteria, as shown in Figure 8, demonstrating that the proposed coatings were more efficient in controlling the bacterial growth of the *S. aureus* strains. The same was reported by Doudstar et al.[28] in systems containing PCL+TTO, and this fact may be associated with the structure of *E. coli*, which has a lipid bilayer (cell membrane and specific external membrane) providing better protection of the bacterial cell against external antibacterial agents.

HA-coated titanium implants have been used as vehicles for drugs or other bioactive molecules that have been shown to promote osseointegration and bone growth, in addition to reducing the potential for bacterial infection[60-63].

Dudek-Wicher et al.[54] verified that the presence of intrinsic porosity in CaP favors the chemisorption of actives when they compared the adherence dynamics of terpinen-4-ol present in TTO to the HA or agar surfaces, confirming that the substance penetrates better in the channels of the porous HA-disks.

The same positive effect was observed by Alves et al.[41] for bioceramic scaffolds based on β-TCP, in which the addition of TTO in the coatings provided significant antibacterial activity, in addition to a slow release of the active, as can be suggested for the systems proposed in this work (Ti+PCL+TTO and Ti+HA+PCL+TTO).

4. Conclusion

The proposed coatings increase the bioactivity of TiCP when compared to metallic substrate without coating.

The micrographs obtained for the Ti+PCL+TTO and Ti+HA+PCL+TTO samples after the bioactivity test demonstrate the evolution of the apatite layer, with homogeneous growth during the four weeks for both conditions, although more accelerated for the condition with previous HA coating. Furthermore, the formed apatites presented an appreciable globular structure for the osseointegrative process. The TTO incorporated into the coating had a desirable effect on the morphology of the apatite granules formed during the bioactivity tests. The FTIR spectra revealed an increase in the intensity of the CO_3^{2-} and PO_4^{3-} bands, indicating the growth of the bioceramic layer as well as confirmation of a polymeric coating due to the presence of the PCL and TTO characteristic bands. The incorporation of TTO in the proposed coatings provided antimicrobial activity against the strains of bacteria used, being more efficient in controlling the growth of the *S. aureus* strain. In this way, the proposed systems present desirable characteristics for application in medical implants, supporting their potential to enhance the osseointegration process.

5. Acknowledgements

The authors thank the Brazilian research funding agencies FAPEMIG, FAPESP, CNPq, FINEP, and CAPES for the financial support.

6. References

1. Sharma GK, Kukshal V, Shekhawat D, Patnaik A. Fabrication and characterization of metallic biomaterials in medical applications. In: Patnaik A, Banerjee MK, Kozeschnik E, Cavaleiro A, Davim JP, Kukshal V, editors. Advanced materials and manufacturing processes. Boca Raton: CRC Press; 2021. p. 95-105.
2. Silva MHP. Osteoinductive biomaterials. In: Olabi AG, editor. Encyclopedia of smart materials. Amsterdam: Elsevier; 2016. p. 507-511.
3. Melnik EV, Filonov MR, Litvinova LS, Khlusov IA, Koroleva ES, Tverdokhlebov SI, et al. In vitro degradation behaviour of hybrid electrospun scaffolds of polycaprolactone and strontium-containing hydroxyapatite microparticles. Polym Degrad Stabil. 2019;167:21-32.
4. Glazov IE, Belyavskaya VA, Luginina TS, Shupletsova VV, Mazurov DV, Smirnov VM, et al. Effect of platelet-poor plasma additive on the formation of biocompatible calcium phosphates. Mater Today Commun. 2021;27:102224.
5. Collins MN, Ren G, Young K, Pina S, Reis RL, Oliveira JM. Scaffold fabrication technologies and structure/function properties in bone tissue engineering. Adv Funct Mater. 2021;31(21):2010609.
6. Frassica MT, Grunlan MA. Perspectives on synthetic materials to guide tissue regeneration for osteochondral defect repair. ACS Biomater Sci Eng. 2020;6:4324-36.
7. Wang T, Ren X, Bai Y, Liu L, Wu G. Adhesive and tough hydrogels promoted by quaternary chitosan for strain sensor. Carbohydr Polym. 2021;254:117298.
8. Singh N, Batra U, Kumar K, Mahapatro A. Investigating TiO2–HA–PCL hybrid coating as an efficient corrosion resistant barrier of ZM21 Mg alloy. J Magnes Alloy. 2021;9:627-46.
9. Kiran A, Kumar TS, Sanghavi R, Doble M, Ramakrishna S. Antibacterial and bioactive surface modifications of titanium implants by PCL/TiO2 nanocomposite coatings. Nanomaterials (Basel). 2018;8:860.
10. Vu AA, Bose S. Natural antibiotic oregano in hydroxyapatite-coated titanium reduces osteoclastic bone resorption for orthopedic and dental applications. ACS Appl Mater Interfaces. 2020;12:52383-92.
11. Filipović U, Dahmane RG, Ghannouchi S, Zore A, Bohinc K. Bacterial adhesion on orthopedic implants. Adv Colloid Interface Sci. 2020;283:102228.
12. Khatoon Z, McTiernan CD, Suuronen EJ, Mah TF, Alarcon EI. Bacterial biofilm formation on implantable devices and approaches to its treatment and prevention. Heliyon. 2018;4(12):e01067.
13. Raphel J, Holodniy M, Goodman SB, Heilshorn SC. Multifunctional coatings to simultaneously promote osseointegration and prevent infection of orthopaedic implants. Biomaterials. 2016;84:301-14.
14. Bazaka O, Jacob MV, Crawford RJ, Ivanova EP. Effect of titanium surface topography on plasma deposition of antibacterial polymer coatings. Appl Surf Sci. 2020;521:146375.
15. Low WL, Kenward K, Britland ST, Amin MC, Martin C. Essential oils and metal ions as alternative antimicrobial agents: a focus on tea tree oil and silver. Int Wound J. 2017;14:369-84.
16. Khatoon UT, Nageswara Rao GVS, Mohan KM, Ramanaviciene A, Ramanavicius A. Antibacterial and antifungal activity of silver nanospheres synthesized by tri-sodium citrate assisted chemical approach. Vacuum. 2017;146:259-65.
17. Khatoon UT, Rao GVSN, Mohan MK, Ramanaviciene A, Ramanavicius A. Comparative study of antifungal activity of silver and gold nanoparticles synthesized by facile chemical approach. J Environ Chem Eng. 2018;6:5837-44.
18. Mirzaei R, Ranjbar R, Aliahmadi A, Ghaffari S, Moghaddam G, Rezaei A, et al. The biofilm-associated bacterial infections unrelated to indwelling devices. IUBMB Life. 2020;72:1271-85.
19. Chen P, Shen Y, Jin H, Lin S, Peng Q, Ding Y. Fabrication of a silver nanoparticle-coated collagen membrane with anti-bacterial and anti-inflammatory activities for guided bone regeneration. Biomed Mater. 2018;13:065014.
20. Ferreira CC, Alves APN, Sousa LL, Pires TM, Cordeiro R, Aguiar A, et al. Titanium biomimetically coated with hydroxyapatite, silver nitrate and polycaprolactone, for use in biomaterials (biomedicine). Mater Res. 2019;22:e20190177.
21. Ferreira CC, Sousa LL, Barboza CS, Marques RFC, Mariano NA. Modifications in the surface of titanium substrate and the incorporation of an essential oil for biomaterial application. J Mater Eng Perform. 2023;32:6759-69.
22. Sousa LL, Ferreira CC, Alves APN, Barboza CS, Silva RF, Silva DL. Titanium coating with hydroxyapatite and chitosan doped with silver nitrate. Mater Res. 2018;20:863-8.
23. Hzounda Fokou JB, Jazet Dongmo PM, Boyom FF. Essential oil's chemical composition and pharmacological properties. In: El-Shemy HA, editor. Oils of nature – essential oils. London: IntechOpen; 2020. p. 1-20.
24. Mugao LG, Gichimu BM, Muturi PW, Mukono ST. Characterization of the volatile components of essential oils of selected plants in Kenya. Biochem Res Int. 2020;2020:1-8.
25. Maquera-Huacho PM, Villanueva ME, Romero AI, Quispe Rojas Y, Lobato MF, Vázquez B, et al. In vitro antibacterial and cytotoxic activities of carvacrol and terpinen-4-ol against biofilm formation on titanium implant surfaces. Biofouling. 2018;34:699-709.
26. Puvača N, Čabarkapa I, Bursić V, Petrović A, Aćimović M. Antimicrobial, antioxidant and acaricidal properties of tea tree (Melaleuca alternifolia). Technol Eng Manag. 2018;1:29-38.
27. Sánchez-González L, Vargas M, González-Martínez C, Chiralt A, Cháfer M. Characterization of edible films based on hydroxypropylmethylcellulose and tea tree essential oil. Food Hydrocoll. 2009;23:2102-9.
28. Doustdar F, Ramezani S, Ghorbani M, Mortazavi Moghadam F. Optimization and characterization of a novel tea tree oil-integrated poly(ε-caprolactone)/soy protein isolate electrospun mat as a wound care system. Int J Pharm. 2022;627:122218.
29. Mielczarek M, Gilewicz A, Mielczarek K, Niemirowicz-Laskowska K, Deptuła P, Tokajuk G, et al. Effect of tea tree oil

addition on the microstructure, structure and selected properties of chitosan-based coatings electrophoretically deposited on zirconium alloy substrates. Appl Surf Sci. 2023;609:155266.
30. ASTM: American Society for Testing and Material. ASTM F67-06: Standard specification for unalloyed titanium, for surgical implant applications. West Conshohocken: ASTM International; 2006.
31. ISO: International Organization for Standardization. ISO 23317: Implants for surgery – In vitro evaluation for apatite-forming ability of implant materials. Geneva: ISO; 2014.
32. Ferreira CC, Pires TM, Silva RF, Alves APN, Sousa LL, Cordeiro R, et al. Improvement of titanium corrosion resistance by coating with poly-caprolactone and poly-caprolactone/titanium dioxide: potential application in heart valves. Mater Res. 2018;20:126-33.
33. Coelho MFC, Cordeiro JM, Ribeiro KRA, Lemos CA, Ferreira CV, Rocha LA, et al. Biomimetic coating on titanium: evaluation of bioactivity and corrosion. Mater Res Express. 2019;6:126505.
34. Kokubo T, Yamaguchi S. Novel bioactive materials developed by simulated body fluid evaluation: surface-modified Ti metal and its alloys. Acta Biomater. 2016;44:16-30.
35. CLSI: Clinical and Laboratory Standards Institute. Performance standards for antimicrobial disk susceptibility tests. 13th ed. Wayne, PA: CLSI; 2018. CLSI document M02.
36. Eraković S, Matković A, Matković T, Grubač Z, Šegota S, Ivanković M, et al. Corrosion stability and bioactivity in simulated body fluid of silver/hydroxyapatite and silver/hydroxyapatite/lignin coatings on titanium obtained by electrophoretic deposition. J Phys Chem B. 2013;117:1633-43.
37. Kokubo T, Yamaguchi S. Novel bioactive materials developed by simulated body fluid evaluation: surface-modified Ti metal and its alloys. Acta Biomater. 2016;44:16-30.
38. Wang S, Ma D, Wu W, Han Y, Guan J, Liu S, et al. Tuning pore features of mineralized collagen/PCL scaffolds for cranial bone regeneration in a rat model. Mater Sci Eng C. 2020;106:110186.
39. Safari B, Aghazadeh M, Roshangar L, Aghanejad A, Davaran S. A bioactive porous scaffold containing collagen/phosphorous-modified polycaprolactone for osteogenesis of adipose-derived mesenchymal stem cells. Eur Polym J. 2022;171:111220.
40. Costa BD, Tavares LE, Junqueira RG, Mello AFM, Almeida AL. Neoformação óssea e osteointegração de biomateriais micro e nanoestruturados em ovinos. Pesq Vet Bras. 2015;35(2):177-87.
41. Alves APN, Ferreira CC, Sousa LL, Pires TM, Barboza CS, Oliveira RCR, et al. 3D-printed β-TCP/S53P4 bioactive glass scaffolds coated with tea tree oil: coating optimization, in vitro bioactivity and antibacterial properties. J Biomed Mater Res B Appl Biomater. 2023;111:881-94.
42. Sabbieti MG, Agas D, Maggi F, Vittori S, Marchetti L. Molecular mediators involved in *Ferulago campestris* essential oil effects on osteoblast metabolism. J Cell Biochem. 2011;112:3742-54.
43. Elbahnasawy AS, Valeeva ER, El-Sayed EM, Rakhimov II. The impact of thyme and rosemary on prevention of osteoporosis in rats. J Nutr Metab. 2019;2019:1-10.
44. Gorodzha SN, Tikhonov AA, Kharin MI, Frolova AA, Kiseleva EP, Bukharova TB, et al. Investigation of the morphology and structure of porous hybrid 3D scaffolds based on polycaprolactone involving silicate-containing hydroxyapatite. J Surf Invest X-ray, Synchrotron Neutron Tech. 2018;12:717-26.
45. Glazov IE, Krut'ko VK, Musskaya ON, Kulak AI. Calcium phosphate apatites: wet formation, thermal transformations, terminology, and identification. Russ J Inorg Chem. 2022;67:173-82.
46. Dorozhkin SV. Calcium orthophosphates. Biomatter. 2011;1:121-64.
47. Dorozhkin SV, Epple M. Biological and medical significance of calcium phosphates. Angew Chem Int Ed. 2002;41:3130-46.
48. Catauro M, Papale F, Bollino F. Characterization and biological properties of TiO2/PCL hybrid layers prepared via sol-gel dip coating for surface modification of titanium implants. J Non-Cryst Solids. 2015;415:9-15.
49. Chen CM, Chen SM, Lin SF, Liang HC, Wu CC. Clinical efficacy of polycaprolactone β-calcium triphosphate composite for osteoconduction in rabbit bone defect model. Polymers (Basel). 2021;13(15):2552.
50. Tabatabaei F, Gelin A, Rasoulianboroujeni M, Tayebi L. Coating of 3D printed PCL/TCP scaffolds using homogenized-fibrillated collagen. Colloids Surf B Biointerfaces. 2022;217:112670.
51. Lee S, Choi D, Shim JH, Nam W. Efficacy of three-dimensionally printed polycaprolactone/beta tricalcium phosphate scaffold on mandibular reconstruction. Sci Rep. 2020;10:4979.
52. Helaehil JV, de Oliveira RS, Oliveira FA, Silva RB, Araújo IB, Mansur AAP, et al. In vivo investigation of polymer-ceramic PCL/HA and PCL/β-TCP 3D composite scaffolds and electrical stimulation for bone regeneration. Polymers (Basel). 2022;14:65.
53. Valente FL, Fonseca LC, Motta LH, Dell'Aqua CP, Oliveira RC, Franco JS, et al. Hydroxyapatite, polycaprolactone and alendronate composites for bone regeneration in rabbits' olecranon: histological features. Arq Bras Med Vet Zootec. 2016;68:543-7.
54. Dudek-Wicher R, Junka A, Paleczny J, Bartoszewicz M. Activity of liquid and volatile fractions of essential oils against biofilm formed by selected reference strains on polystyrene and hydroxyapatite surfaces. Pathogens. 2021;10(5):515.
55. Weng S, Liu S, Qian Y, Huang W, Li Z, Deng Y, et al. Synthesis, characterization, antibacterial activity in dark and in vitro cytocompatibility of Ag-incorporated TiO2 microspheres with high specific surface area. J Mater Sci Mater Med. 2018;29(5):50.
56. Visai L, De Nardo L, Punta C, Melone L, Cigada A, Imbriani M, et al. Titanium oxide antibacterial surfaces in biomedical devices. Int J Artif Organs. 2011;34:929-46.
57. Dicastillo CL, Correa MG, Martínez FB, Streitt C, Galotto MJ. Antimicrobial effect of titanium dioxide nanoparticles. In: Mareș M, Lim HE, Lai KS, Cristina RT, editors. Antimicrobial resistance – a one health perspective. London: IntechOpen; 2021. p. 1-18.
58. Mumu SK, Hossain MM. Antimicrobial activity of tea tree oil against pathogenic bacteria and comparison of its effectiveness with eucalyptus oil, lemongrass oil and conventional antibiotics. Am J Microbiol Res. 2018;6:73-8.
59. Singh BR, Vadhana P, Bhardwaj M, Kumar V. Comparative antimicrobial activity of tea tree oil (Melaleuca oil) and common topical antimicrobials against bacteria associated with wound and topical infections. Pharm Anal Acta. 2016;7(11):1000513.
60. Maher S, Mazinani A, Barati MR, Losic D. Engineered titanium implants for localized drug delivery: recent advances and perspectives of titania nanotubes arrays. Expert Opin Drug Deliv. 2018;15:1021-37.
61. Tejero R, Anitua E, Orive G. Toward the biomimetic implant surface: biopolymers on titanium-based implants for bone regeneration. Prog Polym Sci. 2014;39:1406-47.
62. Schmidmaier G, Wildemann B, Bail HJ, Lucke M, Fuchs T, Stemberger A, et al. Bone morphogenetic protein-2 coating of titanium implants increases biomechanical strength and accelerates bone remodeling in fracture treatment: a biomechanical and histological study in rats. Bone. 2002;30:816-22.
63. Manam NS, Harun WSW, Shri DHA, Ghani SA, Kurniawan T, Ismail MHI, et al. Study of corrosion in biocompatible metals for implants: a review. J Alloys Compd. 2017;701:698-715.